Dynamics of a semiconductor laser with optical feedback

G. Huyet,[1] J. K. White,[2] A. J. Kent,[1] S. P. Hegarty,[1] J. V. Moloney,[1,2] and J. G. McInerney[1,2]
[1]*Physics Department, National University of Ireland, University College, Cork, Ireland*
[2]*Arizona Center for Mathematical Sciences, University of Arizona, Tucson, Arizona 85721*
(Received 18 June 1998; revised manuscript received 28 January 1999)

We investigate both experimentally and theoretically the dynamics of a semiconductor laser with optical feedback in the low-frequency fluctuation regime. First we demonstrate that low-frequency fluctuations can be observed for both single and multimode operation of a semiconductor laser with optical feedback. The analysis of the fast dynamics associated with this low-frequency instability is well described by single-mode rate equations. In the multimode regime, fast pulsation is observed in every laser mode. In this case the fluctuations in total intensity are much smaller than those in the intensity of each individual mode. This indicates the presence of anticorrelations dynamics at high frequency between the different laser modes.
[S1050-2947(99)08307-9]

PACS number(s): 42.65.Sf, 05.45.−a, 42.55.Px

Time-delayed dynamical systems have been the subject of much research in nonlinear dynamics [1–4]. In optics, these equations have been considered in order to describe external cavity lasers [5,6]. In this experiment, an external reflector reinjects the light into the main laser resonator. This system, which was first conceived to stabilize semiconductor lasers, displays a rich variety of instabilities. For example, several routes to chaos [7,8] were identified when the amount of light reinjected into the cavity (the feedback level) is small and/or for short external cavity length (small delay time). For longer external cavities and/or larger feedback levels, the laser output displays deep power dropouts at a frequency much lower than the external cavity frequency and the internal laser relaxation oscillation frequency. For this reason this instability is usually referred to as low-frequency fluctuation (LFF). Although this instability has been observed for over 20 years [9], it remains only partially understood.

The external cavity experiment is commonly described by the Lang-Kobayashi (LK) equations [5] for a single-mode laser under the presence of optical feedback. These equations describe the evolution of the complex amplitude of this laser mode and the carrier density. The effect of the external cavity is incorporated by the addition of the time-delayed electric field amplitude. Numerical simulations of these equations have shown a low-frequency evolution similar to that experimentally observed [10]. Further numerical simulations [11] have also shown the presence of fast continuously pulsating operation of the laser intensity during the LFF regime. This fast dynamics was first observed using a streak camera [12], which showed pulses in a time window of a few external cavity round-trip times. However, it was also observed that the LFF regime always appears together with multimode operation [13] of the laser diode. In this case, the probability distribution of the fast dynamics differs from pulses [14]. A detailed analysis of the temporal evolution of the laser intensity just after a power dropout revealed a close analogy with the turn-on transient of a semiconductor laser [15]. This phenomenon was explained as the result of an interferometric effect of the laser diode cavity. Due to the increase in carrier number at dropout, the refractive index decreases and thus shifts the cavity modes. The frequency of the gain curve peak may also vary with the carrier density. This causes the light in the external cavity to be off-resonance with the laser diode cavity and to be reflected strongly. Since the laser is impervious to the light in the external cavity immediately after the dropout, it recovers in the same fashion as a gain switched laser, where many modes are activated following the switch-on since they all initially have gain. In a gain-switched laser they will generally compete leading to a single-mode state. In an external cavity semiconductor laser the interaction between the diode laser modes may be affected by the optical feedback and multiple diode-laser-mode emission may occur. Recent measurements of the laser dynamics with a streak camera [16] have pointed out a partial locking between the different laser modes just before a dropout. From their result, the authors inferred that LFF may originate from the multimode behavior of the laser.

Here, we demonstrate that LFF may be observed with both single-mode and multimode operation. We first confined the dynamics to a single laser mode and showed that we were able to recover the high-frequency pulses predicted by the LK model. However, without this confinement the laser becomes multimode and the fluctuations in the total intensity are much smaller than those measured in a single mode. This indicates the presence of strong anticorrelation between the different modes at high frequency. This behavior, which is similar to antiphase dynamics observed in different dynamical systems [17–21] is supported by numerical simulations of a system of coupled nonlinear partial differential equations describing the experiment. This demonstrates both numerically and experimentally that without this confinement the different laser modes operate out of phase at high frequency, obscuring fast pulses present in individual modes in the total intensity.

The experimental arrangement was similar to that in Ref. [14]. It consisted of a Hitachi HLP 1400 semiconductor laser that emits light from both facets. The light from one facet was focused onto an external high reflector and reinjected into the laser cavity, forming a 50 cm external cavity. A variable neutral density filter placed in the external cavity

allowed control of the feedback level. The light from the other facet was used for analysis. One portion of this light was used to study the fast dynamics by coupling to a high-speed dc-coupled photodiode with temporal resolution of 20 ps, which was in turn connected to a sampling oscilloscope with an equivalent bandwidth of 22 GHz. By triggering the oscilloscope on a signal unrelated to the laser intensity large sets of randomly sampled data were acquired and used to construct the intensity histogram from dc to 15 GHz. The remainder of the light from this facet was coupled to an optical spectrum analyzer and to a low-frequency photodetector connected to a 500 MHz real-time oscilloscope for characterization of the low-frequency time series.

In order to study the multimode versus single-mode behavior of the system we can also insert etalons to filter the feedback signal and/or the detected signal. An etalon (finesse $=15$, FSR$=2$ THz) in the external cavity restricts feedback to just a single mode. Although this etalon favors one particular mode, it does not guarantee single-mode emission. A second etalon (finesse$=32$, FSR$=1$ THz) placed before the fast photodiode allows analysis of the dynamics of each laser mode individually. With the etalon in the external cavity, we are able to observe power dropouts both above and below solitary laser threshold. When the laser is pumped above threshold the etalon does not suppress multimode dynamics entirely: at the dropout event latent laser modes are excited [13,22]. Below the solitary laser threshold however, these latent modes are not excited and the laser operates with a single mode, allowing a true comparison with the rate equation model. In what follows we will concentrate on the below-threshold regime. We will contrast the single-mode dynamics of the external cavity, including the etalon with the multimode dynamics of the empty external cavity for the same parameter values (i.e., the same external cavity length, threshold reduction, and injection current).

Figure 1 shows the measured low-frequency time traces of the total intensity of multimode LFF (top), of one mode from the multimode LFF (center), and the total intensity for single-mode LFF obtained with the intracavity etalon (bottom). We note that it has been shown in Ref. [13] that the laser modes switch off together and the laser recovers in multiple modes. Nevertheless, Fig. 1 shows that the temporal evolution of one mode does not resemble very closely the evolution of the total power. For single-mode LFF the low-frequency time trace is also dissimilar to the multimode case. The mean time between two consecutive power dropouts is smaller (about half) and the low-frequency signal is more noisy than the multimode LFF.

Figure 2 shows the measured probability distribution of the laser intensity for the total power of the multimode LFF, for one mode of the multimode LFF, and for the single-mode LFF. The probability distribution for the single-mode LFF is peaked just above the spontaneous-emission level and decreases monotonically with increasing intensity, indicating the presence of fast pulses predicted by the rate equation model [11], as shown in Fig. 2. It contrasts with the multimode probability distribution, which peaks near the laser mean power and falls off more rapidly at high intensities, indicating that the most probable intensity corresponds to the mean intensity and that the intensity fluctuations are smaller. The probability distribution of just one of the modes differs

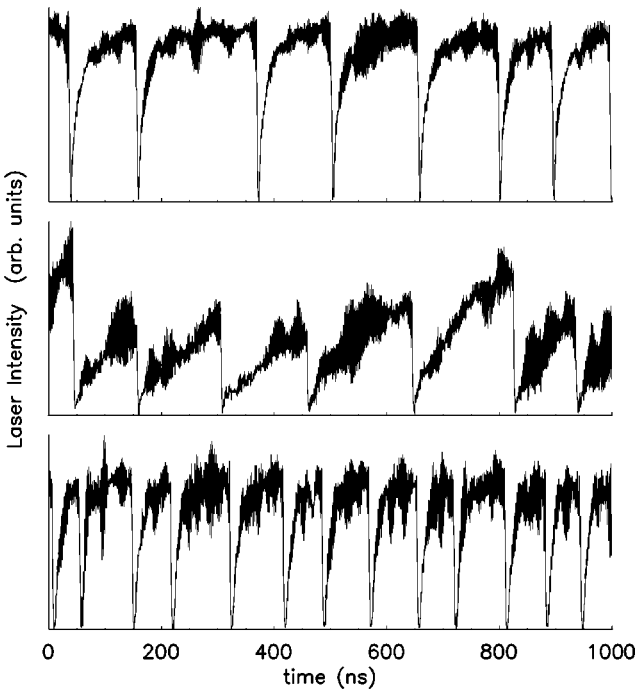

FIG. 1. Low-frequency time traces of the laser intensity observed on a 500-MHz oscilloscope for identical feedback level and injection current. Top, multimode LFF, total intensity; center, multimode LFF, one filtered mode, not taken simultaneously with top trace; bottom, single-mode LFF.

from that of the total intensity and is more like the single-mode LFF distribution. The fluctuations are large and the probability distribution is asymmetric. From these measurements, we conclude that each laser mode exhibits high-amplitude, high-frequency fluctuations not exhibited by the total power. This indicates that the individual laser modes operate in antiphase at high frequency.

To model this experiment, we use a system of partial differential equations with a parabolic gain dispersion [23]:

$$\frac{\partial E^{\pm}}{\partial t} \pm \frac{\partial E^{\pm}}{\partial z} = \kappa \left[(N-1)\left(1 + G_d \frac{\partial^2}{\partial z^2}\right) - i\alpha N - \gamma_{int} \right] E^{\pm}, \tag{1}$$

$$\frac{\partial N}{\partial t} = J - \gamma N - (N-1)[|E^{+}|^2 + |E^{-}|^2],$$

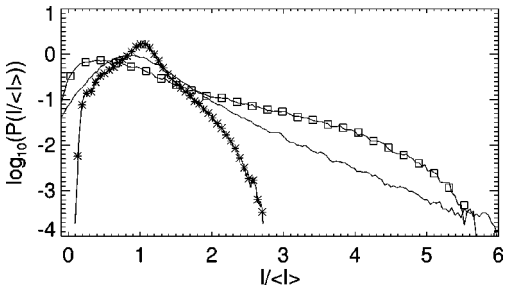

FIG. 2. Measured histogram of the laser intensity with a 0–15 GHz bandwidth. Stars, multimode LFF, total intensity; solid lines, multimode LFF, one filtered mode; squares, single-mode LFF.

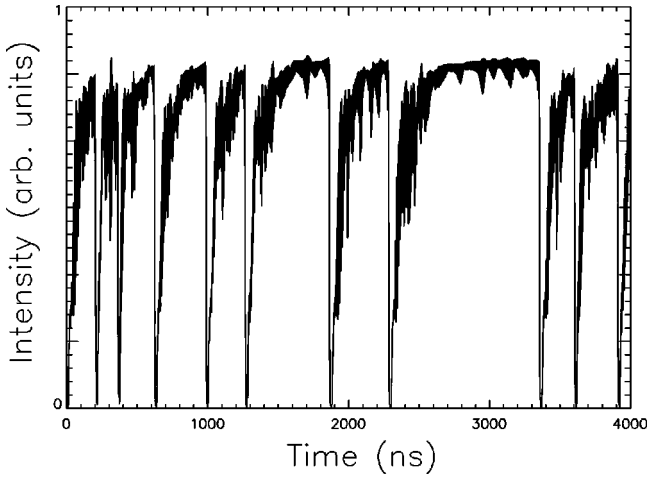

FIG. 3. Total intensity filtered at 500 MHz obtained from numerical simulations. The frequency of the dropouts is lower than in the experiment due to the difference of external cavity length.

with the boundary conditions

$$E^{+}(0,t)=\sqrt{R_1}E^{-}(0,t),$$

$$E^{-}(1,t)=\sqrt{R_2}E^{+}(1,t)+(1-R_2)\times\sum_{n=1}^{\infty}\eta^{n}R_2^{n-1/2}E^{+}(1,t-n\tau), \qquad (2)$$

where $E^{\pm}$ represent the amplitudes of the two counterpropagating waves in the cavity, N is the carrier density, κ is the damping rate of the electric field in the cavity, α is the linewidth enhancement factor (which describes the phase-amplitude coupling), G_d measures the gain linewidth, γ_{int} represents internal nonradiative laser losses, γ is the carrier damping rate, J is the pumping parameter, $R_{1,2}$ are the facet reflectivities, η is the feedback strength, and τ is the external cavity round-trip time. We numerically integrated these equations with parameters typical for semiconductor lasers $\kappa=0.088$, $G_d=4\times10^{-6}$, $\alpha=4$, $\gamma_{int}=0.79$, $R_{1,2}=0.32$, $\gamma=0.0049$, $\eta=0.075$, and $\tau=0.17$ corresponding to 5 ns. For our simulations the laser was biased at solitary laser threshold.

In studying the simulated LFF we filtered the total intensity with a 500-MHz square filter, averaging out the high-frequency fluctuations. The energy is distributed among many modes and we note that all the laser modes switch off together at low frequency (see Fig. 3). Numerical integration of the LK equations with the same parameter values show power dropouts about three times faster than the multimode model, in agreement with the experiment (see Fig. 1). This indicates that multimode behavior acts to stabilize the system and make power dropouts less frequent.

For a more accurate comparison with experiment we have also constructed the intensity histogram. To mimic the experimental detector we applied a 22-GHz square filter to the intensity in each longitudinal mode. Figure 4 shows excellent

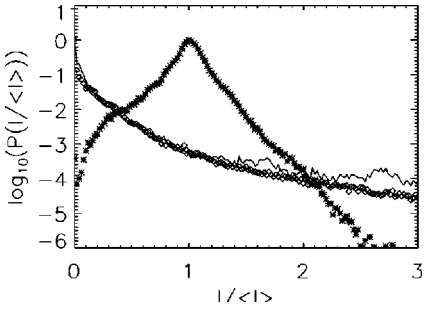

FIG. 4. Histogram of the laser intensity I calculated for the simulation in Fig. 5 using a 22-GHz square filter. Stars, multimode LFF calculated using Eq. (1); solid lines, multimode LFF one filtered mode; squares, single-mode LFF calculated from the LK equations.

agreement between the simulations and experiment, with a strong peak at the mean intensity which rapidly falls off for higher intensities. Additionally, we created a histogram for data calculated from the LK equations (using the same 22 GHz filter). As expected there is no peak at the mean intensity and no rapid falloff at high intensities. Instead the maximum is at the spontaneous emission level (0 in our simulations) with a long tail corresponding to high intensity pulses. The difference between the experimental and numerical probability distributions could be improved by adding spontaneous emission and gain saturation in our numerical simulation. This would alter both low and high intensity probabilities.

The model allows us to look at the fast pulses in greater detail. In Fig. 5 we see the high intensity pulses predicted by the experimental intensity histograms of a single mode and a very clear picture of antiphase dynamics. High intensity pulses in one mode tend to correspond to low intensities in other modes. Energy is exchanged between the modes so that one mode always has a significant intensity and the total intensity is rarely small. The net effect on the total intensity is that there are fast fluctuations about the mean intensity, not pulses as predicted by the LK equations.

In conclusion, we have experimentally demonstrated the existence of fast pulses as predicted by the single-mode LK equations by constraining the dynamics to a single laser mode. We have also demonstrated both theoretically and ex-

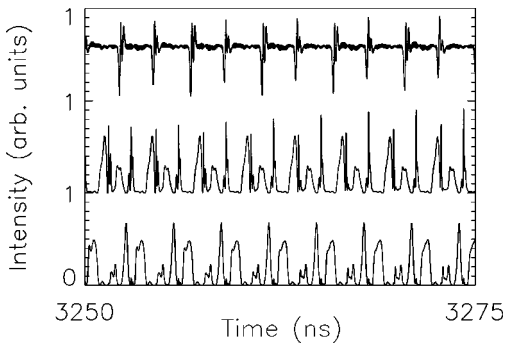

FIG. 5. Energy in the two strongest longitudinal modes from the 30 lasing (bottom and center) and the total intensity (top) from numerical simulations. The time is the same as in Fig. 3. Each mode exhibits pulsed dynamics with the energy oscillating between the two modes. Graphs have been offset for clarity.

perimentally that without this confinement the different laser modes operate out of phase at high frequency, obscuring fast pulses present in individual modes in the total intensity.

We acknowledge R. Gillen for technical support and the Commission of the EU for financial support of two of us (G.H. and A.K.) under the Marie Curie Fellowship Program. J.V.M. and J.K.W. acknowledge support from the U.S. Air Force Office of Scientific Research, U.S. Air Force Materiel Command, USAF, under Grant Nos. AFOSR-97-1-0002 and AFOSR-97-1-0142.

[1] J. Hale, *Theory of Functional Differential Equations* (Springer-Verlag, New York, 1977).
[2] N. Khrustova, G. Veser, A. Mikhailov, and R. Imbihl, Phys. Rev. Lett. **75**, 3564 (1995).
[3] G. Giacomelli and A. Politi, Phys. Rev. Lett. **76**, 2686 (1996).
[4] M. E. Bleich, D. Hocheiser, J. V. Moloney, and J. E. S. Socolar, Phys. Rev. E **55**, 2119 (1997).
[5] R. Lang and K. Kobayashi, IEEE J. Quantum Electron. **QE-16**, 347 (1980).
[6] G. H. M. van Tartwijk and D. Lenstra, Quantum Semiclassic. Opt. **7**, 87 (1995).
[7] J. Moerk, B. Tromborg, and J. Mark, IEEE J. Quantum Electron. **28**, 93 (1992).
[8] J. Ye, H. Li, and J. G. McInerney, Phys. Rev. A **47**, 2249 (1993).
[9] C. Risch and C. Voumard, J. Appl. Phys. **48**, 2083 (1977).
[10] T. Sano, Phys. Rev. A **50**, 2719 (1994).
[11] G. van Tartwijk, A. Levine, and D. Lenstra, IEEE J. Sel. Top. Quantum Electron. **1**, 466 (1995).
[12] I. Fischer, G. van Tartwijk, A. Levine, W. Elsaesser, E. O. Gobel, and D. Lenstra, Phys. Rev. Lett. **76**, 220 (1996).
[13] G. Huyet, S. Balle, M. Giudici, C. Green, G. Giacomelli, and J. R. Tredicce, Opt. Commun. **149**, 341 (1998).
[14] G. Huyet, S. P. Hegarty, M. Giudici, B. de Bruyn, and J. G. McInerney, Europhys. Lett. **40**, 619 (1997).
[15] S. P. Hegarty, G. Huyet, P. Porta, and J. G. McInerney, Opt. Lett. **23**, 1206 (1998).
[16] G. Vaschenko, M. Giudici, J. J. Rocca, C. S. Menoni, J. R. Tredicce, and S. Balle, Phys. Rev. Lett. **81**, 5536 (1998).
[17] P. Hadley and M. R. Beasley, Appl. Phys. Lett. **50**, 621 (1987).
[18] K. Wiesenfeld, C. Bracikowski, G. James, and R. Roy, Phys. Rev. Lett. **65**, 1749 (1990).
[19] K. Otsuka, P. Mandel, S. Bielawski, D. Derozier, and P. Glorieux, Phys. Rev. A **46**, 1692 (1992).
[20] S. Bielawski, D. Derozier, and P. Glorieux, Phys. Rev. A **46**, 2811 (1992).
[21] P. Mandel and J. Wang, Opt. Lett. **19**, 533 (1994).
[22] M. Giudici, L. Giuggioli, C. Green, and J. R. Tredicce, Chaos Solitons Fractals **20**, 811 (1999).
[23] J. K. White, J. V. Moloney, A. Gavrielides, V. Kovanis, A. Hohl, and R. Kalmus, IEEE J. Quantum Electron. **34**, 1469 (1998).